The Astronomical Journal, 129:2400–2410, 2005 May


# THE DETECTION OF ABUNDANCE ANOMALIES IN THE INFRARED SPECTRA OF CATACLYSMIC VARIABLES: SHORTER PERIOD SYSTEMS

Thomas E. Harrison[1,2] and Heather L. Osborne[2]
Department of Astronomy, New Mexico State University, Box 30001, MSC 4500, Las Cruces, NM 88003-8001;
tharriso@nmsu.edu, hosborne@nmsu.edu

and

Steve B. Howell
WIYN Observatory and National Optical Astronomy Observatory, 950 North Cherry Avenue, Tucson, AZ 85719; howell@noao.edu
*Received 2004 November 22; accepted 2005 February 14*

## ABSTRACT

We present *K*-band spectra for 12 cataclysmic variables (CVs) with orbital periods under 6 hr. We confidently detect the secondary stars in nine of these systems and may have detected them in the other three. Nine of the 12 CVs clearly have CO first-overtone absorption features that are weaker than they should be for the derived spectral type. We demonstrate that, in general, the weak CO features are due to a carbon deficiency in the secondary star. In the case of U Gem, UU Aql, and TW Vir the carbon abundance in the secondary star appears to be very low, likely only a few percent of the solar value. Deficits of carbon, when combined with the detection of $^{13}$CO and the ultraviolet detections of enhanced levels of nitrogen in other CV systems, imply that material that has been processed through the CNO cycle is finding its way into the photospheres of CV secondary stars. While several plausible models exist to explain unusual levels of CNO species in CV secondary stars, they do not detail how such species as aluminum, magnesium, or silicon (elements that show abundance anomalies in our spectra) will behave. It appears that the standard model for the formation and evolution of CVs needs substantial revision.

*Key words:* binaries: close — novae, cataclysmic variables — stars: abundances — stars: evolution

## 1. INTRODUCTION

In Harrison et al. (2004d, hereafter Paper I) we presented infrared spectra of long-period ($P_{\rm orb} > 6$ hr) cataclysmic variables (CVs). Here we present *K*-band spectra for 12 CVs with $1.89 \leq P_{\rm orb} \leq 5.25$ hr. CVs are short-period binary systems consisting of white dwarf primaries that are accreting material via Roche lobe overflow from low-mass, late-type secondary stars. The standard paradigm for the evolutionary history of CVs suggests that long-period systems have spent less time as a CV, have lost less mass, and are less "bloated" than their short-period counterparts (see Howell et al. 2001). The standard theory also proposes that the majority of CV secondary stars were still on the main sequence when initial contact occurred and mass transfer began (Howell 2001). In Paper I, however, we found that the infrared spectra of long-period CVs show peculiar abundance patterns, most notably weak CO features and probable enhancements of $^{13}$CO. That finding is consistent with CNO-processed material being present in the atmospheres of those secondary stars, and seems to reinforce recent results from UV spectroscopy that have found strong enhancements of nitrogen and deficits of carbon (Gänsicke et al. 2003). It appears that at some time during the history of these CVs, either an epoch of CNO processing has occurred within the secondary star itself, or enriched material from the current primary found its way into the atmosphere of the secondary star.

If the secondary stars of short-period systems have been losing mass for a longer time than their long-period cousins, they might show even more extreme abundance patterns. Below, we present *K*-band spectra of 12 short-period CV systems. Nine of the 12 systems show weaker than expected CO features. In addition, we find evidence for apparent deficits and/or enhancements for a number of other common elements. In § 2 we discuss our observations, followed by a description of the spectra of the objects in § 3, followed by our conclusions in § 4.

## 2. OBSERVATIONS

The infrared spectroscopy for the program objects was obtained using SpeX[3] on the Infrared Telescope Facility (IRTF) on Mauna Kea during two different observing runs and at the Cerro Tololo Inter-American Observatory (CTIO) using OSIRIS[4] on the Blanco 4 m Telescope. The IRTF runs occurred on 2002 April 6 and 7 and 2003 May 16–19. The OSIRIS observations were obtained on 2002 March 20 and 21. Both instruments were used in the mode that provided the highest possible resolution in the *K* band. For SpeX, this consisted of using the spectrograph in single-order mode with a 0.″3 slit, giving a dispersion of 5.51 Å pixel$^{-1}$. The spectra produced in this mode covered the entire *K* band, from 1.96 to 2.50 $\mu$m. OSIRIS was also used in single-order, long-slit mode, with a 0.″5 slit, the f/7 camera, and the grating in third order. The resulting dispersion was 3.70 Å pixel$^{-1}$. We selected the grating angle to cover the spectral region from 2.09 to 2.40 $\mu$m. For the CTIO run, the conditions were photometric and the seeing was excellent (with an average FWHM

[1] Visiting Astronomer, Kitt Peak National Observatory, National Optical Astronomy Observatory, which is operated by the Association of Universities for Research in Astronomy, Inc., under cooperative agreement with the National Science Foundation (NSF).

[2] Visiting Astronomer at the Infrared Telescope Facility, which is operated by the University of Hawaii under contract from NASA.

[3] For more on SpeX, see http://irtfweb.ifa.hawaii.edu/Facility/spex.

[4] For more on OSIRIS, see http://www.ctio.noao.edu/instruments/ir_instruments/osiris/index.html.

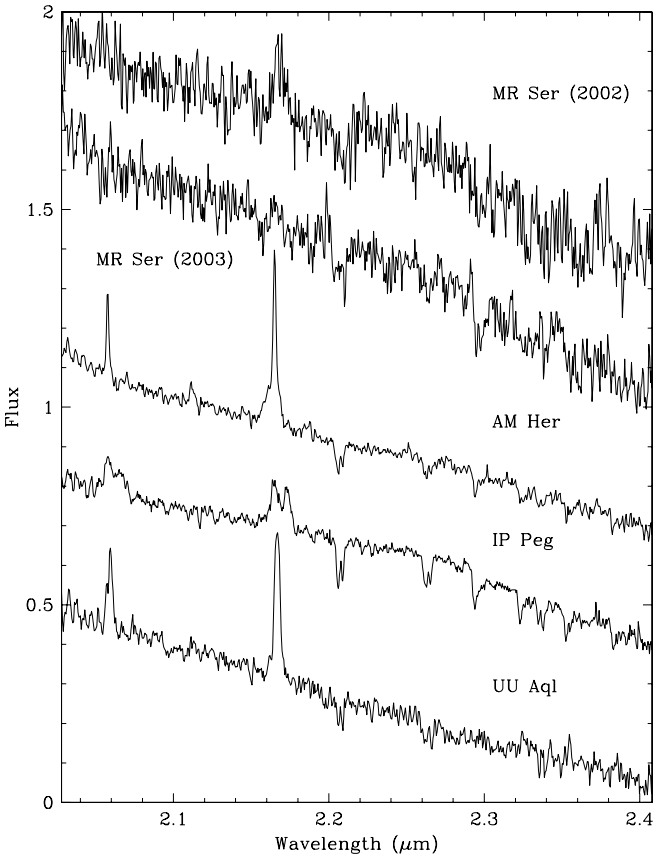


FIG. 1.—Unsmoothed *K*-band spectra for MR Ser, AM Her, IP Peg, and UU Aql. Except for IP Peg, which was observed using NIRSPEC on Keck II, these spectra were obtained using SpeX on the IRTF. MR Ser was observed on both 2002 February and 2003 May. The data have been reduced as described in the text, and the orbital motion of the secondary star has been removed using published ephemerides.

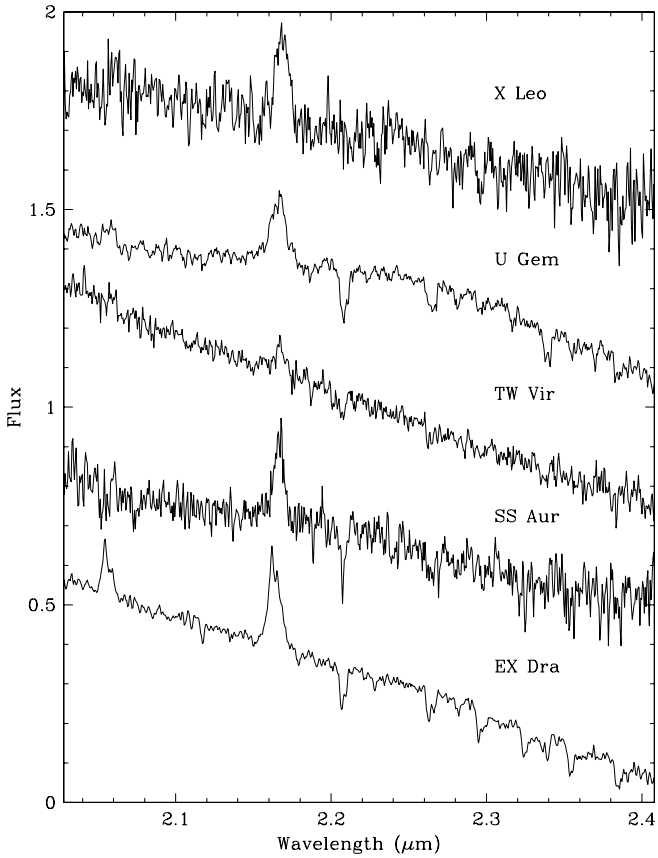


FIG. 2.—Spectra of X Leo, U Gem, TW Vir, SS Aur, and EX Dra, as in Fig. 1; however, all of the data presented here were obtained using SpeX on the IRTF.

near 0.″5). Unfortunately, the conditions at the IRTF were nonphotometric except for the second half of the last night.

The observing procedure was nearly identical for all runs. The spectra obtained with OSIRIS used a script that took five individual exposures along the slit, each separated from the preceding by 8″. For just about all the CVs, the exposure times were 4 minutes in length. For the data obtained using SpeX a similar observing routine, but one in which data were obtained at six separate positions along the slit, was employed. Typical exposure times with SpeX were 3 minutes. Total on-source exposure times ranged from about 12 minutes in the case of AM Her to several hours in the case of MR Ser. For all of the program objects, observations of nearby early A and G dwarf stars were obtained just before or after the observational sequence for each target. The observations of the A and G dwarf stars were used to correct the spectra of the program objects for telluric effects. Finally, observations of a number of bright, late-type stars were obtained to act as spectral-type templates. While the exposure times for these bright objects were quite short, the same scripts as used for the CV observations were employed. For a full discussion of the reduction process for SpeX and OSIRIS data, see Paper I.

In addition to the CV spectra obtained with SpeX and OSIRIS, below we include a spectrum of IP Peg obtained using NIRSPEC[5] on the Keck II telescope in photometric conditions on 2003 September 6 (see Howell et al. 2004 for further details). We used NIRSPEC in the low-resolution mode with a 0.″38 slit. The grating tilt was set to cover the wavelength region from 2.00 to 2.42 $\mu$m, with a dispersion of 4.27 Å pixel$^{-1}$. We employed the four-nod script and obtained eight spectra with 2 minute exposure times. The NIRSPEC data were reduced in the same fashion as the SpeX and OSIRIS data.

The final, fully reduced spectra for MR Ser, AM Her, IP Peg, and UU Aql are shown in Figure 1. Those for X Leo, U Gem, TW Vir, SS Aur, and EX Dra are shown in Figure 2. The spectra obtained using OSIRIS (CZ Ori, TW Vir, BD Pav, and RR Pic) are shown in Figure 3. As described in Paper I, there remains some low-level fringing in the OSIRIS spectra, confined to the region between 2.21 and 2.26 $\mu$m, that we were unable to remove. We present the unsmoothed spectra in these figures so that the reader can determine the noise level and the strength and/or reality of various features as ascertained from the smoothed spectra of the individual CVs to be discussed in § 3. A journal of our observations is presented in Table 1.

### 2.1. *Accounting for Orbital "Smearing"*

Because of the faintness of the program CVs and the long observing sequences necessary to obtain useful data, the production of a final spectrum can be compromised by the orbital motion of the secondary star. This is especially true for the short-period systems discussed here. To properly account for the orbital smearing, we require an accurate spectroscopic ephemeris for the CV and the Doppler correction of each individual spectrum before a final spectrum can be produced from their median. We have listed the orbital phase coverage for the program objects in Table 1. For UU Aql and TW Vir such ephemerides do

[5] Information on the NIRSPEC instrument can be found at http://www2.keck.hawaii.edu/inst/nirspec/nirspec.html.

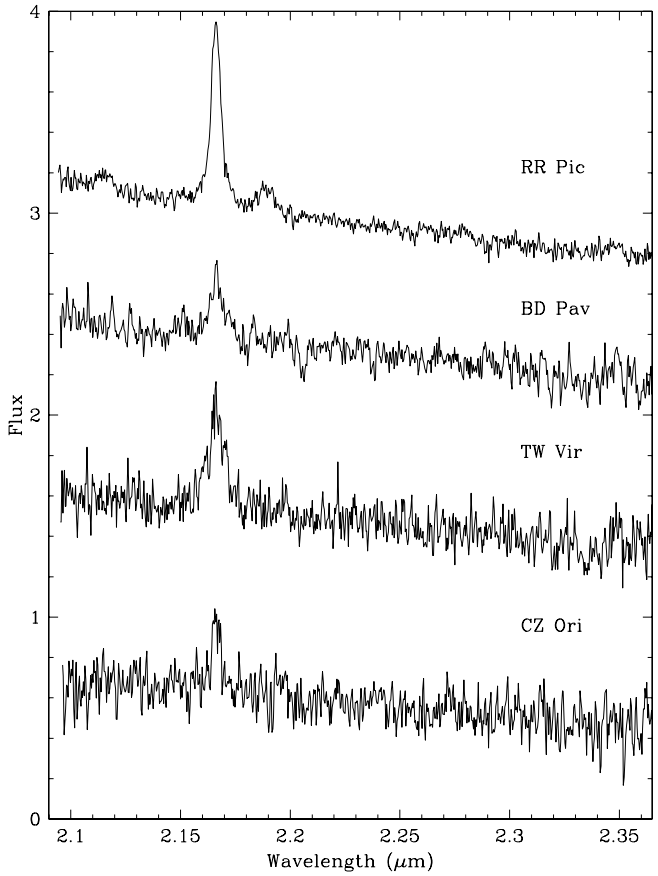


FIG. 3.—Spectra for RR Pic, BD Pav, TW Vir, and CZ Ori obtained using OSIRIS on the Blanco 4 m Telescope.

not exist, and thus only the percentage of an orbital period covered by our observations is listed. For MR Ser, data were obtained on multiple nights, and on each of those nights more than one complete orbit was observed.

Given an accurate ephemeris, it is rather easy to correct the spectra for the orbital motion. For these short-period systems, the orbital motion of the secondary can be significant. For example, the radial velocity semiamplitude for MR Ser is $K_2 = 165$ km s$^{-1}$. Thus, to correct for this motion each spectrum was individually extracted, and wavelength calibrated using an argon arc lamp. Then each of these spectra was divided by the most appropriate standard star to remove the telluric features. The orbital phase of each spectrum was determined, and the estimated radial velocity was removed using the IRAF *dopcor* package. Once all the spectra for a particular object were Doppler-corrected, they were medianed together to form the final spectrum. In the case of RR Pic, a phasing and estimate of the system parameters exists but an actual radial velocity curve for the secondary star does not. We have made an estimate for the secondary star's motion in RR Pic using the published parameters of the system and Doppler-corrected the data to produce a median spectrum. For UU Aql and TW Vir, the final spectra are simple medians without any correction for the motion of the secondary star.

## 3. THE INFRARED SPECTRA

In what follows, we describe the *K*-band spectra for each individual object. In nearly all cases, the spectra that were presented in Figures 1–3 have been smoothed to improve their signal-to-noise ratios (S/Ns). We compare the smoothed CV spectra to those of identically smoothed spectral templates that we have obtained with SpeX. Examples of the *K*-band spectra for several late-type dwarfs are presented in Figure 4, along with line identifications for the strongest absorption features. In our spectral analysis, we have used *K*-band line identifications from Wallace et al. (1996) and Hinkle et al. (1995). For each of the CVs, we have rotationally broadened the spectral type templates to match the observed, or predicted, rotational broadening of the secondary star. As described in Paper I, we visually compared the strength of nearby spectral features in the CV spectra to the same features in the templates, as is the procedure for normal MK spectral classification. The use of nearby spectral features alleviates issues that arise because of contamination. As shown in Figure 4, the strengths of most of the atomic features rapidly weaken with decreasing temperature. This is especially true for Mg I and Al I in late M dwarfs. However, the reverse is true for Na I, the first-overtone features of CO, and water vapor for the spectral range encountered here.

For several of the CVs presented below, it is obvious that the *K*-band spectra are significantly bluer than the spectra of the late-type template stars. This is different from the results we found in Paper I, where systems with strong accretion disk emission, such

TABLE 1
OBSERVATION JOURNAL

| Object | Instrument | Obs. Date | Start (UT) | Stop (UT) | Phase |
|---|---|---|---|---|---|
| CZ Ori..... | OSIRIS | 2002 Feb 21 | 1:08 | 2:17 | 0.81–0.03 |
| EX Dra..... | SpeX | 2003 May 17 | 10:19 | 11:01 | 0.26–0.39 |
| SS Aur..... | SpeX | 2002 Apr 8 | 5:30 | 7:14 | 0.76–0.15 |
| TW Vir..... | OSIRIS | 2002 Feb 21 | 7:04 | 9:16 | 45% |
| TW Vir..... | SpeX | 2003 May 18 | 7:04 | 8:09 | 25% |
| BD Pav..... | OSIRIS | 2002 Feb 22 | 8:53 | 9:38 | 0.87–0.03 |
| U Gem..... | SpeX | 2002 Apr 8 | 7:38 | 8:45 | 0.05–0.31 |
| X Leo ..... | SpeX | 2002 Apr 8 | 9:22 | 11:03 | 0.61–0.04 |
| UU Aql ..... | SpeX | 2003 May 18 | 13:21 | 14:26 | 28% |
| IP Peg..... | NIRSPEC | 2003 Sep 6 | 9:19 | 9:32 | 0.69–0.74 |
| RR Pic..... | OSIRIS | 2002 Feb 22 | 3:36 | 4:22 | 0.45–0.65 |
| AM Her..... | SpeX | 2003 May 17 | 11:15 | 11:29 | 0.94–0.00 |
| MR Ser..... | SpeX | 2002 Feb 7 | 12:29 | 14:46 | 121% |
| MR Ser..... | SpeX | 2002 Feb 8 | 11:25 | 14:10 | 145% |
| MR Ser..... | SpeX | 2003 May 20 | 7:22 | 10:02 | 141% |

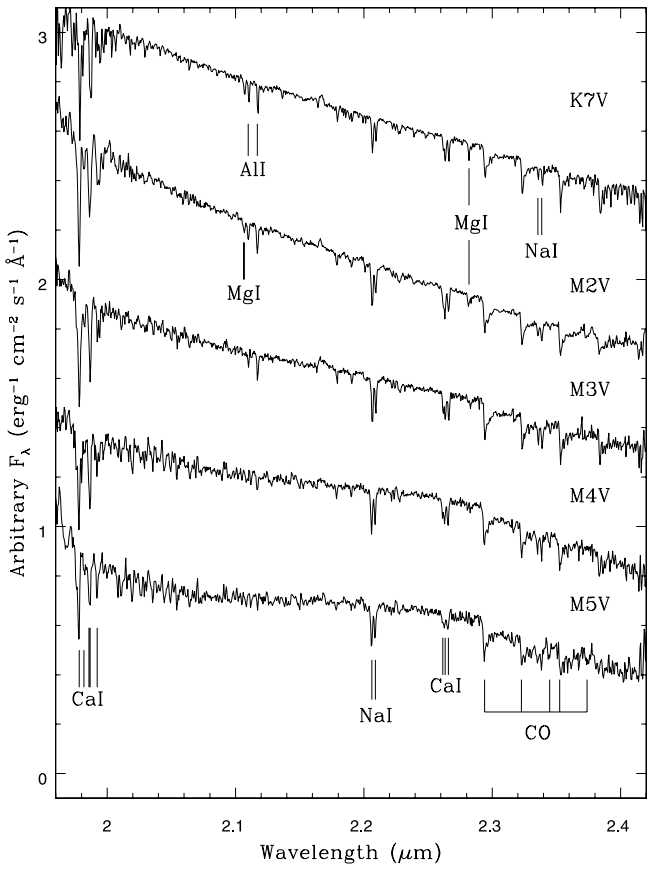


FIG. 4.—*K*-band spectra for some of the late-type stars used as templates for spectral classification of the CV spectra. The most prominent and important spectral lines used for classification are identified. Except for Na I, all of these strong lines weaken with decreasing temperature. The molecular features due to the first-overtone features of CO and those from water vapor increase in depth as we progress to later types. The clear change in slope in the stellar continuum near M4/5 V is due to water vapor.

as SS Cyg, were found to have slightly redder continuua than the templates. As discussed in Paper I, a hot blackbody source has a steeper continuum than the standard (predicted) accretion disk spectrum. Thus, the subtraction of a hot blackbody will redden the CV spectrum much more quickly than would the subtraction of a flatter spectrum source and result in the assumption of the lowest level of contamination. We make no claim for the validity of this process, letting the results speak for themselves. We order the following discussion by orbital period from the longest to shortest.

### 3.1. *CZ Orionis*

CZ Ori has an orbital period of 5.254 hr and $K_{2MASS} = 12.27$. As reported by Osborne et al. (2002), CZ Ori has a spectral energy distribution that is consistent with, and dominated by, an early M-type dwarf. However, time-resolved infrared photometry of CZ Ori does not reveal significant ellipsoidal variations. They conclude that its orbital inclination is $i \leq 25^\circ$. Using this inclination and the data listed in the Ritter-Kolb CV catalog (Ritter & Kolb 2003), we have estimated $V_{rot} \sin i = 65$ km s$^{-1}$ and applied this amount of broadening to our template spectra. The AAVSO online database indicates that CZ Ori was near minimum light at the time of our observations, although it did go into outburst 3 days later. Fifteen 4 minute exposures were obtained and combined to produce the spectrum shown in Figure 5, where we compare it to an M0 V and an M3 V.

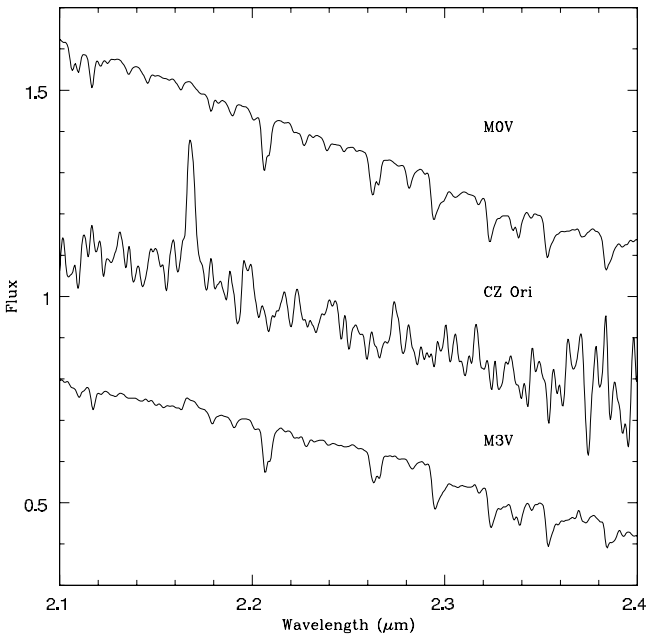


FIG. 5.—Smoothed (to 40 Å pixel$^{-1}$) spectrum of CZ Ori compared to rotationally broadened and smoothed spectra of M0 V and M3 V templates.

The OSIRIS spectrum of CZ Ori is much too poor to extract useful constraints on the spectral type or any possible abundance anomalies. There are features consistent with the positions of both Na I doublets, but there is no clear evidence for CO absorption features. The slope of the continuum matches the M3 V template quite well but, as we found for the longer period CVs in Paper I, systems with significant accretion disk contamination have flatter spectral slopes than K and M dwarfs, so it is possible that the spectral type of the secondary star in CZ Ori is earlier than M3.

### 3.2. *EX Draconis*

EX Dra is a bright ($K_{2MASS} = 12.04$), eclipsing dwarf nova with an orbital period of $P_{orb} = 5.038$ hr. Baptista et al. (2000) found that the masses of the two components in the binary were $M_1 = 0.75\,M_\odot$ and $M_2 = 0.54\,M_\odot$. Using these values, we estimate a rotational velocity of $V_{rot} \sin i = 137$ km s$^{-1}$ for the secondary star, and our template spectra have been broadened accordingly. The spectrum, shown in Figure 5, is the median of 12 3 minute exposures obtained with SpeX. At the time of our observations, EX Dra had $m_V \sim 14$, on the decline from an outburst that had occurred 2 weeks earlier. The spectrum of EX Dra is fairly normal, with a continuum that is consistent with a late K dwarf. In Figure 6 we compare the spectrum of EX Dra to the spectra of a K5 V and a K7 V. The slope of the continuum and the strengths of the Na I and Ca I features in the spectrum EX Dra are an excellent match to the same features in the K7 template, consistent with the results of Baptista et al. Throughout the spectrum, the lines from Mg I are weaker than expected. There is a hint that the lines from Ni I and Sc I are slightly stronger than those in the K7 V template. The two Al I lines at 2.110 and 2.117 $\mu$m appear to be somewhat weaker than expected but could be contaminated by He I emission at 2.113 $\mu$m, since the 2.059 $\mu$m line of He I is quite strong. The CO features in the spectrum of EX Dra are weaker than those seen in the template stars. In addition, the line profiles in the spectrum of EX Dra appear to be quite a bit broader than those of the broadened template spectra. When medianing together a large number of spectra, the absorption lines from the CV secondary can be artificially

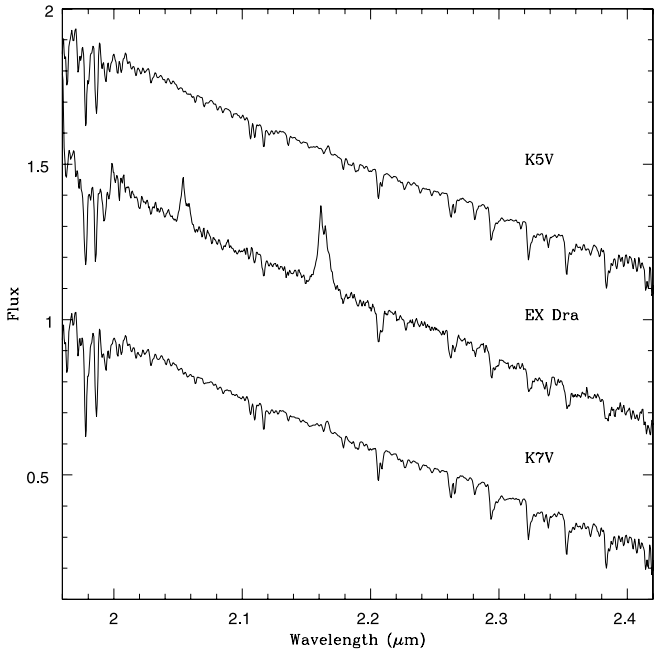


FIG. 6.—Unsmoothed spectrum of EX Dra compared to K5 V and K7 V templates.

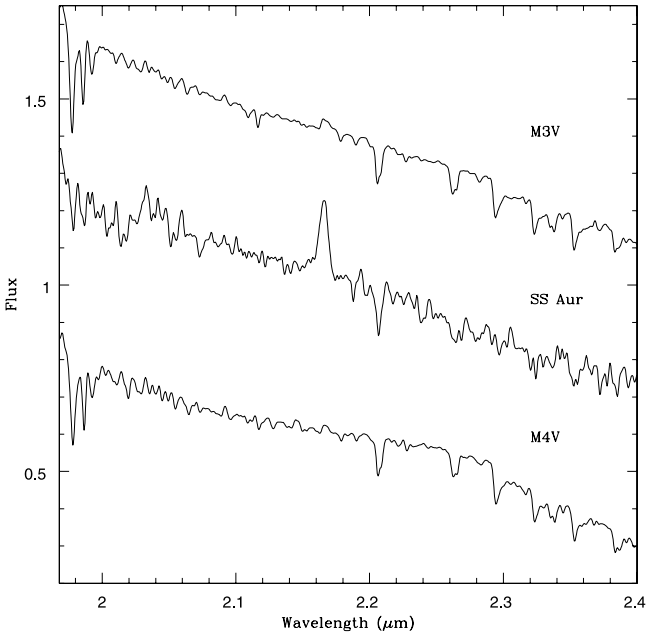


FIG. 7.—Smoothed (to 40 Å pixel$^{-1}$) spectrum of SS Aur compared to properly broadened and smoothed M3 V and M4 V templates.

broadened by using an overestimated value for $K_2$ or via improper phasing. However, since the time required to obtain a good spectrum for EX Dra was very short relative to its orbital period, it appears that we have underestimated $V_{\rm rot} \sin i$. A value of $V_{\rm rot} \sin i = 175$ km s$^{-1}$ provides a better match to the observed spectrum. This value for $V_{\rm rot} \sin i$ would imply a larger value for both $q$ ($\gtrsim$0.9) and $M_1$ ($\gtrsim 1\ M_\odot$).

### 3.3. *SS Aurigae*

A *K*-band spectrum of SS Aur has been presented in Harrison et al. (2000), where a spectral type of M2 $\pm$ 1 was derived. The combination of their photometry and parallax suggested a spectral type near M1 V (assuming a normal main-sequence-type star), consistent with the results of Friend et al. (1990). SS Aur has an orbital period of 4.287 $\pm$ 0.002 hr (Shafter & Harkness 1986). Friend et al. have used time-resolved optical spectroscopy to determine the first orbital parameter solution for SS Aur, find a mass ratio of $q = 0.40 \pm 0.06$, and quote an orbital inclination range of $32^\circ \leq i \leq 47^\circ$. *Preliminary* modeling of the infrared ellipsoidal variations by Osborne et al. (2002) found an orbital inclination of $i = 30^\circ$ for SS Aur. The combination of this value for the inclination and the solution by Friend et al. indicate a secondary star mass near $M_2 = 0.6\ M_\odot$, more appropriate to the mass of a K7 dwarf. Using this mass for $M_2$, the value of $K_2$ from Friend et al., and $i = 30^\circ$, we estimated $V_{\rm rot} \sin i = 123$ km s$^{-1}$ for the secondary star and broadened our template star spectra accordingly. Using the ephemerides of Friend et al., our observations were centered near inferior conjunction, covering the orbital phase range $0.76 \leq \phi \leq 0.15$.

The spectrum of SS Aur, shown in Figure 7, is the median of 24 3 minute exposures. The AAVSO database shows that SS Aur was at minimum light, with the last outburst having occurred 1 month prior to our observations. The spectrum is noisier than desired, but careful analysis reveals that several anomalies are clearly present. The continuum of SS Aur matches that of the M3 V template quite well, although the strong set of Ca I lines centered near 1.98 $\mu$m are somewhat shallower than those found in our template spectra. The telluric correction in this region is significant, and with the inadequate S/N of the SS Aur spectrum the true continuum level in the region of these lines might not be properly corrected. Alternatively, there could be significant disk/hot spot contamination that dilutes the blue end of the *K*-band spectrum. This latter effect would indicate that the secondary star in SS Aur is somewhat later than M4 (as demonstrated in Fig. 4, the Ca I lines weaken with decreasing temperature). Neither the Na I doublet (at 2.20 $\mu$m) nor the Ca I triplet (2.26 $\mu$m) has the proper profiles for an M-type star. On closer examination we find that the Si I lines seem to be much stronger than those of the M-type templates. The Si I lines at 2.136, 2.188, and 2.267 $\mu$m seem especially prominent. It is, in fact, the latter that is partially responsible for the abnormal profile of the Ca I triplet. In addition, there is a pair of Si I lines at 2.207 and 2.208 $\mu$m that increases the depth of the Na I doublet, making this feature appear slightly deeper/sharper than it would normally. It also appears that iron is slightly enhanced, although at a lower level than silicon. The main anomaly in the spectrum of SS Aur is the weakness of the CO features. While the S/N of the spectrum of SS Aur is rather poor beyond 2.28 $\mu$m, if CO was present at its normal level the overtone features would be clearly visible. While there are absorption features consistent with the positions of the main overtone band heads of CO in SS Aur, they are very weak.

### 3.4. *TW Virginis*

TW Vir has a very similar period to SS Aur: $P_{\rm orb} = 4.384$ hr (Shafter 1983). Mateo et al. (1985) detected strong infrared ellipsoidal variations from which they concluded a spectral type of M3 $\pm$ 1 and that the secondary star supplies $\geq$71% of the *K*-band flux. Connon Smith et al. (1997) detected the secondary in the red optical and estimated a spectral type between M5 and M6. Using the data for TW Vir from the Ritter-Kolb catalog, we estimated a $V_{\rm rot} \sin i = 87$ km s$^{-1}$ and applied this broadening to our templates. We observed TW Vir with both OSIRIS and SpeX. The SpeX data, shown in Figure 8, are clearly superior to those obtained with OSIRIS. At the time of the SpeX observations, the AAVSO database had TW Vir at $V = 15.5$. One day later, TW Vir went into outburst, peaking in brightness on

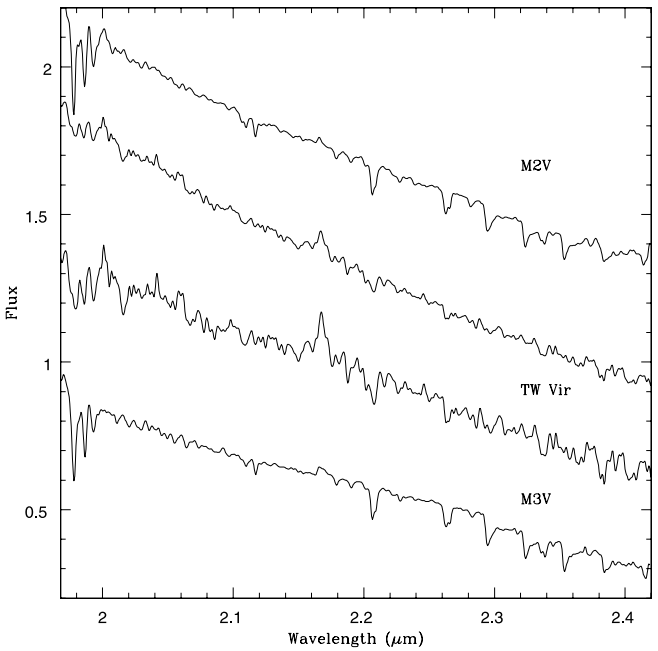


FIG. 8.—Observed spectrum and blackbody-subtracted spectra for TW Vir compared to those of an M2 V and an M3 V star. All spectra have been smoothed to 40 Å pixel$^{-1}$. The blackbody-subtracted spectrum clearly shows the strong set of Ca I lines near 1.98 $\mu$m.

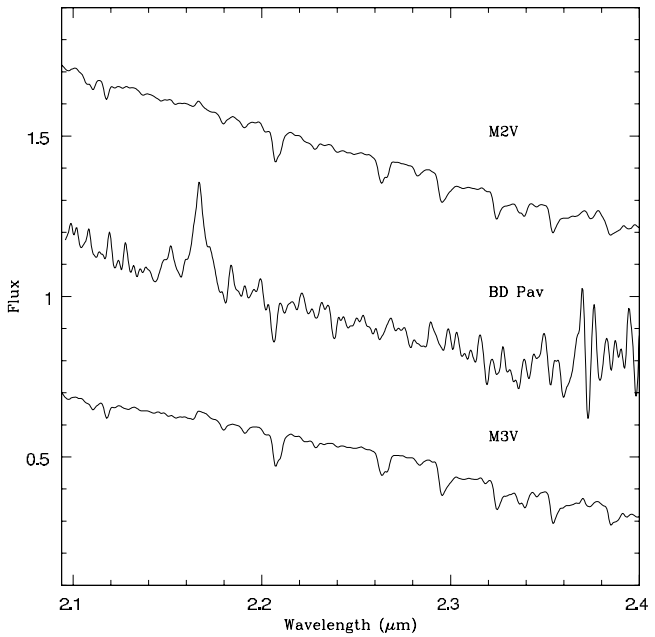


FIG. 9.—OSIRIS spectrum of BD Pav, smoothed to 40 Å pixel$^{-1}$, compared to those of an M2 V and an M3 V star.

20 May 2003. TW Vir has a relatively blue continuum, and we found that the removal of a 20,000 K blackbody that supplied ≈50% of the *K*-band flux creates a spectrum that is a fair match to an M-type continuum. This is a somewhat greater level of contamination than that estimated by Mateo et al. (1985).

The strong contamination of the secondary star spectrum by the accretion disk makes the derivation of information about the secondary star somewhat uncertain. Subtraction of the hot blackbody results in a spectrum that has the slope of an M3 V star. After this subtraction, however, the strong Ca I lines near 1.98 $\mu$m are still not as deep as those seen in the M3 V template. Given the nature of the telluric correction in this region and the low S/N of our TW Vir spectrum, it is easy to understand this result. Taken at face value, however, it suggests that the secondary star in TW Vir (like SS Aur) might be significantly later than M3, requiring the contaminating source to supply a larger percentage of the *K*-band flux. However, the subtraction of such a source results in overly strong Na I and Ca I features. While the spectrum is quite noisy, it does appears that Si is slightly enhanced. The CO overtone features, however, are very weak.

### 3.5. *BD Pavonis*

From the Ritter-Kolb catalog, the parameters for BD Pav are $P_{\rm orb} = 4.305$ hr, $q = 0.63$, and $i = 71^\circ$. These parameters allow us to estimate that the line-of-sight orbital rotation velocity of the secondary star should be $V_{\rm rot} \sin i = 150$ km s$^{-1}$. Friend et al. (1990) obtained a well-sampled radial velocity curve that indicates a secondary star mass near 0.4 $M_\odot$. They derived a spectral type of K7/M1. At the time of our OSIRIS observations the AAVSO light curve shows that BD Pav had $m_V \sim 15$, with the most recent outburst occurring some 3 weeks prior to our observations. As shown in Figure 9, the *K*-band spectrum of BD Pav is slightly bluer than the M-type dwarfs expected at this orbital period. This result is consistent with its infrared colors [$(J-K)_{\rm 2MASS} = 0.58$, $(H-K)_{\rm 2MASS} = 0.11$], which if ascribed solely to the secondary star would indicate a spectral type near K2 V. *Without subtracting any contamination, however, the two* Na I *doublets indicate a spectral type near M3.* To get the continuum of the spectrum of BD Pav to match that of a mid- to late-type M dwarf requires the subtraction of a 20,000 K blackbody that supplies ≈50% of the *K*-band flux. When this operation is performed, the blue Na I doublet becomes extremely strong, even deeper than that of an M8 V!

Given the poor quality of its spectrum, not very much can be derived about BD Pav; however, it does appear that a mid to late M-type star best matches the observed spectrum. This differs from the K7/M1 classification by Friend et al. (1990) on the basis of the Na I doublet at 8190 Å.

### 3.6. *U Geminorum*

U Gem is very well known, and the *K*-band spectrum presented by Harrison et al. (2000) indicated a spectral type of M4, similar to previous estimates made using optical spectroscopy. Harrison et al. noted, however, that the 2.294 $\mu$m CO absorption feature was very weak. The orbital period for U Gem is 4.246 hr, and Smak (2001) lists the other parameters for the U Gem system from which we derive a secondary star rotational velocity of $V_{\rm rot} \sin i = 119$ km s$^{-1}$; this amount of broadening was applied to our template spectra. Our spectrum of U Gem, obtained with SpeX, is shown in Figure 10 and is the median of 18 3 minute exposures. At the time of these observations, U Gem was at minimum light, with the last outburst having occurred 40 days earlier.

The continuum of U Gem closely matches that of the M4 V template. The 2.059 $\mu$m emission line of He I is present but weak. The match of the two Na I doublets and the Ca I triplet in U Gem to the M4 V template spectrum is also excellent, although both appear significantly broader than the same features in the template. We found (see Fig. 10) that to match the profiles of these features required broadening the template spectra to $V \sin i \geq 175$ km s$^{-1}$. An M4 V spectral type implies extraordinarily weak $^{12}$CO features—more like those of a G dwarf than those of an M dwarf! Part of the redward decline in the continuum of M-type stars beyond 2.30 $\mu$m is due to water vapor absorption. It is obvious that the water vapor absorption appears to be normal

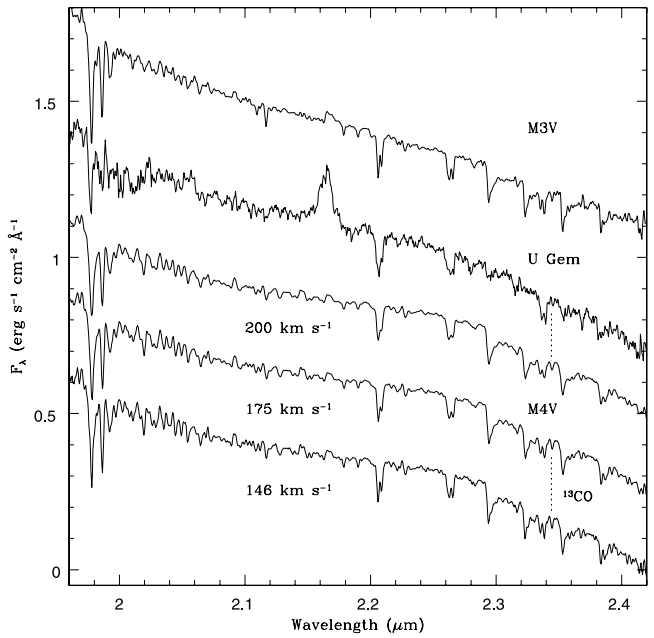


FIG. 10.—Unsmoothed SpeX spectrum of U Gem compared to an M3 V (*top*) and an M4 V (*bottom*) spectrum. The M3 V and bottommost M4 V spectra have been broadened to 146 km s$^{-1}$, the predicted line-of-sight rotational velocity for the secondary star. The profile of the Na I doublet at 2.20 $\mu$m in U Gem indicates a larger rotational velocity, and we present the spectra of an M4 V broadened to both 175 and 200 km s$^{-1}$. The location of the $^{13}$CO band head is indicated.

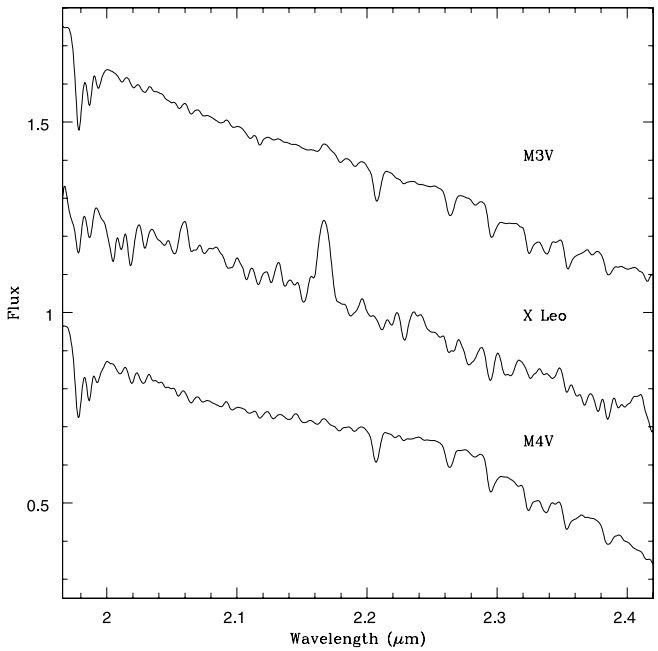


FIG. 11.—Spectrum of X Leo (smoothed to 80 Å pixel$^{-1}$) compared to those of two M dwarfs.

in U Gem, suggesting that a deficit of oxygen cannot explain the weak $^{12}$CO features. It is also apparent in the spectrum for U Gem that a weak $^{13}CO_{(2-1)}$ band head (at 2.345 $\mu$m) is present. It is weaker than the same feature in the M4 V but similar in strength to that seen in the M2 V. This detection is surprising, given the extreme weakness of the $^{12}$CO features. We conclude that $^{13}$CO must be overabundant in the secondary star of U Gem for it to be detected given the weakness of the $^{12}$CO features. Besides enhanced levels of nitrogen and a deficiency of carbon, Long & Gilliland (1999) also found that both silicon and aluminum were underabundant (0.4 × solar) in U Gem. The Al I lines in our *K*-band spectrum for U Gem are quite weak and are consistent with these results. The Si I lines, however, appear to be at their normal strengths for an M4 classification.

### 3.7. *X Leonis*

X Leo is a short-period system, $P_{\rm orb} = 3.946$ hr (Shafter & Harkness 1986), for which the secondary star has not yet been conclusively detected, and insufficient data currently exists to estimate its rotational velocity. The AAVSO database indicates that X Leo had $m_V \sim 16$ at the time of our observations and was declining from an outburst. Because of the faintness of X Leo ($K_{\rm 2MASS} = 13.59$), the poor seeing, and the limited exposure time, the spectrum we obtained with SpeX has very low S/N. Thus, the spectrum had to be smoothed much more than that of any of our other program objects (to 80 Å pixel$^{-1}$), and thus any rotational broadening will not be apparent at such low resolution. The *K*-band spectrum for X Leo presented in Figure 11 shows both He I and H I emission. Given its short period, the expectation is that the secondary star should be a mid to late M-type star. The strong Ca I features near 1.98 $\mu$m are present, confirming the late-type nature of the secondary star. The Ca I triplet near 2.26 $\mu$m is present and has a relatively normal profile. The blue Na I doublet (at 2.20 $\mu$m), however, has a very unusual profile with three well-separated components, none of which have the correct wavelengths. The profile of the redder Na I doublet (at 2.35 $\mu$m) is relatively normal, suggesting that noisy data is partly responsible for the shape of the bluer doublet. Even though the spectrum is rather poor, it is clear that the strongest CO features are present. We conclude that the earliest possible spectral type for the secondary is M2, and given the blue continuum and the likelihood of weaker-than-normal CO features, it probably has a spectral type somewhat later than this.

### 3.8. *UU Aquilae*

UU Aql is a U Gem–type dwarf nova with an orbital period of $P_{\rm orb} = 3.9248$ hr. We observed UU Aql about 1 week after outburst. UU Aql does not have a published ephemeris, so we have listed only the percentage of the orbital period that our observations covered in Table 1. Given the lack of this information, we have broadened our template spectra to estimate $V_{\rm rot} \sin i$ for this object, finding that a value of 100 km s$^{-1}$ provides a good fit to the observed spectrum. The observed, smoothed spectrum, shown in Figure 12, has a continuum that closely matches that of an M2 V. However, if this were the correct spectral type, then all of the absorption features in the spectrum would be much too weak. Thus, we experimented with the subtraction of a hot blackbody and found that the subtraction of one that contributes 50% of the *K*-band flux results in a more realistic set of absorption features, especially the Ca I lines near 1.98 $\mu$m, the depths of which are the most sensitive to a blue contaminating source. After performing this subtraction, analysis of the resulting spectrum shows that all accessible atomic species seem to have the absorption strengths expected for an M4 V. *This is not the case for* CO*, however, which does not appear to be present in this spectrum.* It is true that the S/N at $\lambda > 2.29$ $\mu$m is not especially high, but note that the red Na I doublet (at 2.35 $\mu$m) is clearly seen. UU Aql has the weakest CO features for its spectral type of any CV so far encountered in our survey.

### 3.9. *IP Pegasi*

IP Peg is a bright, famous dwarf nova with an orbital period of $P_{\rm orb} = 3.7969$ hr. We observed IP Peg with Keck, some 70 days

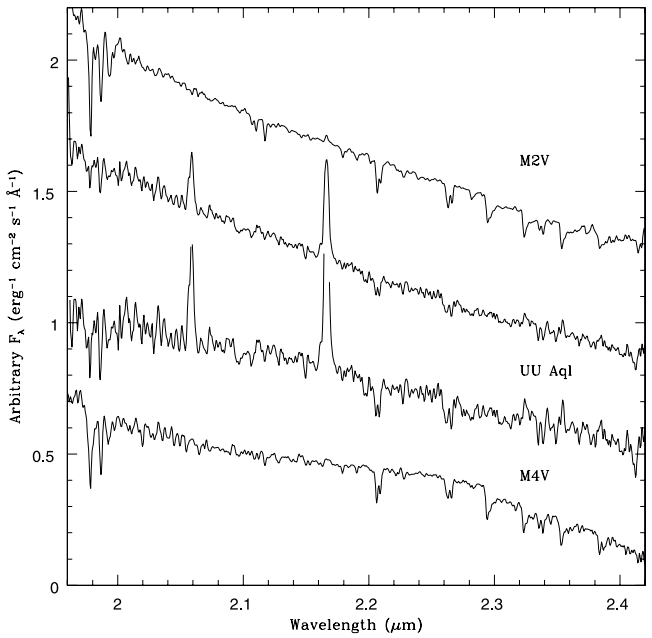


FIG. 12.—Observed and blackbody-subtracted spectra of UU Aql compared to those of an M2 V and an M4 V star.

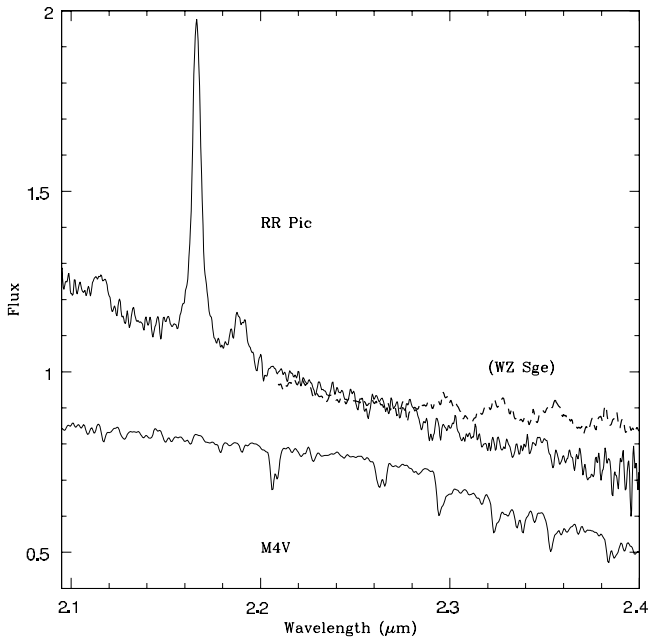


FIG. 14.—Spectrum of RR Pic (smoothed to 20 Å pixel$^{-1}$), showing emission lines of He I at 2.113 $\mu$m, strong H I at 2.166 $\mu$m, and He II at 2.190 $\mu$m. We have superposed a portion of the spectrum of WZ Sge (*dashed line*) from Howell et al. (2004), which has the first-overtone features in emission, to highlight the presence of weak CO absorption features in the spectrum of RR Pic.

after its most recent outburst. The spectrum of IP Peg shown in Figure 13 has been smoothed from the NIRSPEC dispersion of 4.27 Å pixel$^{-1}$ down to that of our templates (5.51 Å pixel$^{-1}$). Watson et al. (2003) have estimated a number of parameters for the IP Peg system from which we derive $V_{\rm rot} \sin i = 144$ km s$^{-1}$. This amount of broadening has been applied to the template star spectra. We cannot identify any significant anomalies in the spectrum of IP Peg.

### 3.10. *RR Pictoris*

RR Pic is the only classical nova in our set of program objects. RR Pic erupted in 1925 and was a slow nova with very strong iron emission lines. It has an orbital period of 3.4806 hr (Haefner & Betzenbichler 1991), an estimated mass ratio of $q = 0.42$, an inclination of $i = 65°$, and $M_1 = 0.95$ (Haefner & Metz 1982). Using these values, we estimate a secondary star rotational velocity of $V_{\rm rot} \sin i = 150$ km s$^{-1}$. The spectrum, presented in Figure 14, shows strong H I Br$\gamma$ emission, as well as emission from He I at 2.113 $\mu$m and He II at 2.190 $\mu$m. The continuum is very blue, and to force it to have the same slope as that of an M-type star requires the subtraction of a hot blackbody that supplies ~80% of the *K*-band continuum! There are no *obvious* absorption features from the secondary star in this system. By comparing the spectrum for RR Pic with that of WZ Sge—which has the CO overtone features in emission—broad, shallow features consistent with the strongest $^{12}$CO features appear to be present. Given the nova outburst and the possibility of deposition of thermonuclear processed material on the secondary star, further spectroscopic investigation of this object at higher resolution is clearly warranted.

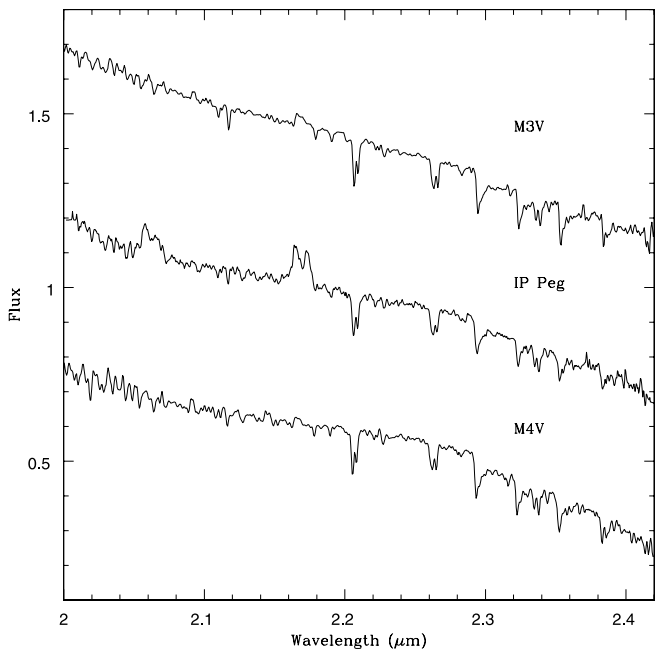


FIG. 13.—Keck II NIRSPEC spectrum of IP Peg compared to those of an M3 V and an M4 V star.

### 3.11. *AM Herculis*

AM Her ($P_{\rm orb} = 3.09$ hr) is the prototype for the magnetic cataclysmic variables in which the magnetic field of the white dwarf primary is strong enough to capture the accretion stream close to the $L_1$ point and the material flows directly on to one (or both) of the magnetic poles without the formation of an accretion disk. Such "polars" occasionally enter very low states, in which the accretion appears to almost stop. The white dwarf in AM Her has a magnetic field strength of $B \sim 13$ MG (Silber et al. 1996). With this field strength, the $n = 4$ cyclotron harmonic, if present, would appear at the blue end of the *K* band. The AAVSO online database indicates that AM Her had $m_V \approx 12.4$ at the time of our observations, putting it in its "high" state. The *K*-band spectrum of AM Her shown in Figure 15 reveals strong, narrow line emission from both He I at 2.059 $\mu$m and H I Br$\gamma$ at 2.166 $\mu$m. In addition, weak He I and He II emission is present at 2.113 and 2.190 $\mu$m, respectively. Southwell et al. (1995) have published a

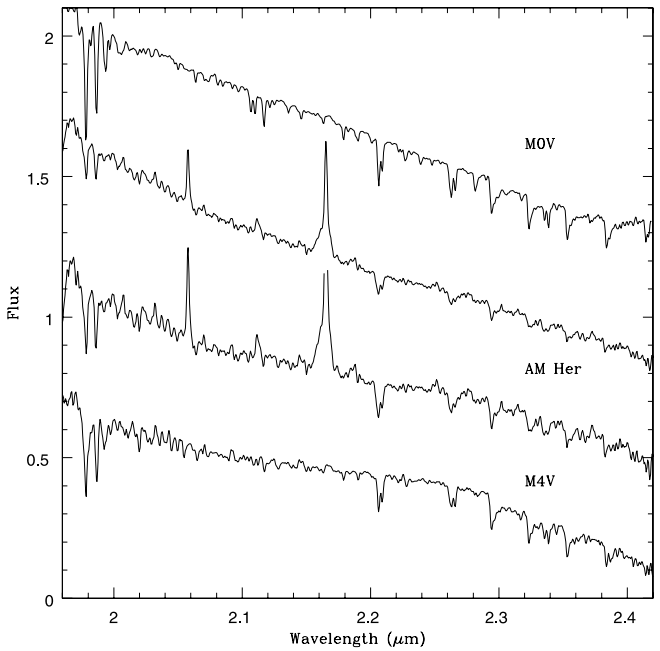


FIG. 15.—Observed and blackbody-subtracted spectra of AM Her (smoothed to 20 Å pixel$^{-1}$) compared to those of an M0 V and an M4 V star.

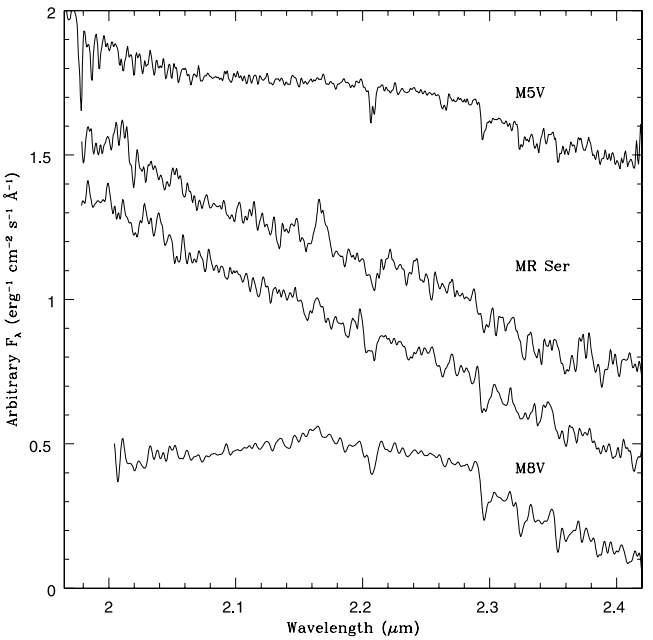


FIG. 16.—Spectra of MR Ser in both 2002 (*second from top*) and 2003 (*third from top*) compared to the *K*-band spectra of an M5 V (*top*) and an M8 V (*bottom*) star. All spectra have been smoothed to 40 Å pixel$^{-1}$.

rotational velocity for the secondary in AM Her of $V_{\rm rot} \sin i = 92 \pm 9$ km s$^{-1}$, and we have applied this broadening to the template spectra shown in Figure 14. The continuum of AM Her is well matched by that of the M0 V template, but like UU Aql none of the absorption features have the proper strengths for such a spectral type. Thus, we have subtracted a hot blackbody that supplies 40% of the *K*-band flux from the spectrum of AM Her. After this subtraction both the continuum and line strengths closely match the spectrum of our M4 V template. This is consistent with the spectral type commonly reported for the secondary star of AM Her (see Szkody et al. 1982, and references therein). A clear indicator that the spectral type of the secondary star in AM Her is later than M0 is provided by the Mg I absorption feature located at 2.281 $\mu$m. This absorption line is strong in K and early M dwarfs but declines rapidly with decreasing temperature, becoming difficult to detect at spectral types of M4 V and later (see Fig. 4). The Mg I line at 2.281 $\mu$m is very weak in the spectrum of AM Her. Thus, unless Mg I is highly deficient, the spectral type of AM Her must be later than M2 V. A close comparison of the spectrum of AM Her to the M4 V template reveals no significant abundance anomalies. There is no clear evidence for the $n = 4$ cyclotron harmonic in our *K*-band spectrum of AM Her.

### 3.12. *MR Serpentis*

MR Ser is the shortest period ($P_{\rm orb} = 1.891$ hr; Schwope et al. 1993) system for which we obtained a spectrum. MR Ser is also a polar, with a magnetic field strength near 26 MG (Schwope et al. 1990). At this field strength, the $n = 2$ cyclotron harmonic should appear at the blue end of the *K* band. In the optical, features from both TiO and Na I are seen (Mukai & Charles 1987) and a spectral type of M5/6 has been derived. A radial velocity curve from these lines indicates a secondary star semiamplitude of $K_2 \sim 165$ km s$^{-1}$. Schwope et al. (1990) provide an orbital ephemeris for MR Ser determined using this radial velocity. As shown in Figure 1, we observed MR Ser on two different epochs; the first was in 2002 February and the second in 2003 May. The 2002 February spectrum of MR Ser is the median of data taken on two different nights. On the first night we observed MR Ser for 2.28 hr, covering 1.21 orbital periods, and obtained 30 180 s exposures. On the second night, under slightly better conditions, we observed MR Ser for 2.75 hr, covering 1.45 orbital periods, and obtained 42 separate spectra. On 2003 May 20 we observed MR Ser for 141% of an orbital period, obtaining 42 spectra. As indicated by the weaker H I emission line, MR Ser was in a lower state of activity during the 2003 observations. Doppler correcting both sets of spectra using the ephemeris from Schwope et al. (1990) results in spectra that clearly show the features of the secondary star (Fig. 16).

The continuum slope of the spectrum for MR Ser is quite similar for both epochs and is relatively blue, although the reddest portions of both spectra do not differ too much from those of our late-type templates. In the 2002 data, there appears to be a broad hump centered near 2.02 $\mu$m, consistent with a cyclotron emission feature. Note that these data are the median of nearly three orbital periods; thus, any phase-dependent cyclotron emission, if similar to that seen in systems like EF Eri (see Harrison et al. 2004c), will be washed out. If we assume that the carbon abundance in the secondary star is normal, the depths of the CO features, the weakness of the Ca I triplet, and the strength of the Na I doublet in the "high"-state spectrum suggest that the secondary is at least as late as an M5—although the depth and profile of the Na I doublet at 2.20 $\mu$m in the high-state spectrum more closely matches that seen in the M8 template. The low-state spectrum has a deeper Na I profile, as well as a deeper first-overtone feature (at 2.294 $\mu$m) of CO, consistent with a very late M-type dwarf. Taken together without the removal of any contaminating sources, the two spectra suggest a spectral type near M8. The subtraction of a hot blackbody source does not result in a realistic spectrum. To get the blue side of the *K* band to flatten (or turn over) requires a significant contamination (>50%). However, if such a source is subtracted from the spectrum of MR Ser, the Na I and CO features become implausibly deep. This suggests to us that the *K*-band spectrum shortward of 2.20 $\mu$m is dominated by a cyclotron feature but that this emission does not significantly affect the red end of the spectrum. We conclude that

if the carbon abundance is relatively normal in the secondary star of MR Ser, the spectral type is near M8. It could be somewhat later if there is any sort of deficit of carbon (but not much too later than L0, since the Na I doublet begins to weaken in the early/mid-L dwarfs). Additional, higher S/N observations are clearly warranted but will require an 8–10 m telescope.

## 4. DISCUSSION

In Paper I we presented a *K*-band spectroscopic survey of 12 long-period ($P_{\rm orb} > 6$ hr) CVs and found evidence for a near-universal deficit in the abundance of carbon in their secondary stars as indicated by the weakness of their CO features. Here we have presented *K*-band spectra for 12 short period systems ($1.89 \leq P_{\rm orb} \leq 5.25$ hr) and arrive at a similar result. The CO features are exceptionally weak in U Gem, TW Vir, and UU Aql (and probably in SS Aur). These systems all have orbital periods near 4 hr. As shown in Harrison et al. (2004b), a preliminary model atmosphere for U Gem, constructed using the non-LTE PHOENIX code (Hauschildt et al. 1999), indicates that the carbon abundance in the secondary star of U Gem is only a few percent of the solar value! The shorter period CV systems appear to show even more extreme carbon deficits than their long-period cousins.

That carbon deficits for CVs are common is further bolstered by recent UV spectroscopy. In their ultraviolet survey of CVs, Gänsicke et al. (2003) find that 10%–15% of the CVs with adequate data showed evidence for strong nitrogen enhancements and carbon deficits. In our survey (including only those objects with adequate spectra) we find that 17 of 20 CV secondary stars show clear evidence for weaker than expected CO features. It is possible that in some of the systems irradiation from the white dwarf, hotspot, and/or accretion disk might alter the strengths of these temperature-sensitive molecular features (see Barman et al. 2000, 2002). However, the presence of normal levels of water vapor absorption and the combination of extremely weak CO features with enhanced levels of $^{13}$CO in several systems indicates that this is not a viable explanation. We conclude that CV secondary stars are truly deficient in carbon and that this material is being deposited on the white dwarfs in these systems through the normal mass transfer process.

The combination of deficits of carbon and enhancements of both nitrogen and $^{13}$C indicate that material processed through the CNO cycle is finding its way into the atmospheres of CV secondary stars. As outlined by Marks & Sarna (1998), there are three possible scenarios for achieving this: (1) the accretion of common envelope material, (2) the sweeping-up of classical novae ejecta, and (3) chemical processing inside a massive star due to normal stellar evolution. As Marks & Sarna discuss, very little material is expected to be accreted from novae ejecta because of the small amount ($10^{-4}\,M_\odot$) of mass involved in the outburst. Similarly, very little mass ($\leq 0.1\,M_\odot$) is expected to be accreted during the common envelope phase because of the fact that the accretion rate can be super-Eddington during this time, and as a result the secondary star expands to fill its Roche lobe and returns any accreted material back to the common envelope (Hjellming & Tamm 1991). Marks & Sarna also found that the period between the end of the common envelope phase and the contact phase is so long that any accreted material will be mixed into the secondary star and will be diluted to the point of being undetectable. This leaves the third scenario: normal evolutionary processes in the secondary star produce CNO cycle products, and the layers where this process occurred are revealed because of the stripping of the outer parts of the secondary star after the mass transfer phase begins. The models presented by Marks & Sarna can produce the observed carbon deficits and nitrogen enhancements but require initial masses for the secondary stars of $>1\,M_\odot$. Population synthesis models by Howell et al. (2001) find that very few CVs form with such massive secondary stars.

UV observations of the peculiar CV system AE Aqr by Jameson et al. (1980) reveal an extreme C IV to N V line ratio, the largest of any CV system (Mauche et al. 1997). Recent infrared spectroscopy of this system by Harrison et al. (2004a) show a K-type secondary star that has no detectable CO features! Schenker et al. (2002) propose that AE Aqr has just evolved from a supersoft X-ray binary into a CV. They model this system as one in which mass transfer begins with a mass ratio of $q > 1$ (i.e., the current secondary star is the more massive component at that time) and a period of thermal timescale mass transfer (TTMT) begins at rates high enough to support stable nuclear burning on the white dwarf, producing a supersoft X-ray source. This phase is brief, on the order of $10^7$ yr, after which the system either detaches or evolves into an ordinary CV. Near the end of the TTMT phase, material from the regions near the core where the CNO cycle was active are transferred, and during this time the abundance ratios of C/N and $^{12}$C/$^{13}$C drop by more than an order of magnitude. Clearly this type of evolution is required to explain the results for systems like U Gem. Schenker et al. (2002) note that an enormous range in the levels of carbon depletion can be achieved simply by changing the initial mass of the secondary star.

The results from the UV surveys indicate that only 10%–15% of CVs show large N/C ratios and hence might be products of TTMT evolution. Our results show that the majority of CVs appear to have evolved through the TTMT stage. This implies that current population synthesis models do not correctly produce a sufficient number of high-mass CV progenitors. Confirmation of the exact number of CV systems that show large carbon deficits await better infrared spectra and proper atmosphere models to quantitatively determine the abundance deficits.

While the models just discussed address the abundances of carbon and nitrogen, they do not describe how the abundances of such metals as silicon, aluminum, or magnesium are altered. As reported above, and identified in Paper I, there are a number of CV systems for which anomalous levels of these heavier metals have been noted. Our results for U Gem show that the secondary star is the source for the low observed abundances of aluminum seen in the white dwarf of this system. Our infrared survey has found additional systems in which such anomalies are present, including a magnesium deficiency in EX Dra and SS Cyg. One possible source for peculiar abundances of such species is the red giant phase of the white dwarf progenitor. As shown by Pilachowski et al. (1996) and Kraft et al. (1998), nucleosynthesis in the cores of red giants can produce unusual abundance patterns such as excesses and/or deficits of sodium, magnesium, oxygen, and aluminum. As noted above, however, the amount of mass accretion during the common envelope phase created by the evolution of the current white dwarf is not expected to have resulted in very much processed material accumulating on the secondary star. One radical possibility is that the current secondary star was the original primary, and that it evolved to a white dwarf first, then accumulated enough material during the common envelope phase of the original secondary (current primary) star's evolution to have been reborn. This conjecture has elements of both the "flip-flop" scenario proposed for Algol-type eclipsing binaries and the TMTT phase described above. Whatever the true answer, the standard evolutionary picture for CVs appears to need considerable revision.

This research was performed with funding from NSF grant AST-9986823, which provided T. E. H. with partial support. H. L. O. acknowledges support from a New Mexico Space Grant Consortium fellowship. This research has made use of the NASA/IPAC Infrared Science Archive, which is operated by the Jet Propulsion Laboratory, California Institute of Technology, under contract to NASA. This publication also makes use of data products from the Two Micron All Sky Survey, which is a joint product of the University of Massachusetts and the Infrared Processing and Analysis Center/California Institute of Technology, funded by NASA and the NSF. We would also like to acknowledge use of the AAVSO's online data archive, which was used to examine the outburst states of the program CVs.

REFERENCES

Baptista, R., Catalán, M. S., & Costa, L. 2000, MNRAS, 316, 529
Barman, T. S., Hauschildt, P. H., & Allard, F. 2002, in ASP Conf. Ser. 261, The Physics of Cataclysmic Variables and Related Objects, ed. B. T. Gänsicke, K. Beuermann, & K. Reinsch (San Francisco: ASP), 49
Barman, T. S., Hauschildt, P. H., Short, I. C., & Baron, E. 2000, ApJ, 537, 946
Connon Smith, R., Sarna, M. J., Catalan, M. S., & Jones, D. H. P. 1997, MNRAS, 287, 271
Friend, M. T., Martin, J. S., Connon-Smith, R., & Jones, D. H. P. 1990, MNRAS, 246, 637
Gänsicke, B. T., et al. 2003, ApJ, 594, 443
Haefner, R., & Betzenbichler, W. 1991, Inf. Bull. Variable Stars, 3665, 1
Haefner, R., & Metz, K. 1982, A&A, 109, 171
Harrison, T. E., Howell, S. B., Campbell, R., & Johnson, J. J. 2004a, BAAS, 205, 19.15
Harrison, T. E., Howell, S. B., Johnson, J. J., Osborne, H. L., & Homeier, D. 2004b, Rev. Mexicana Astron. Astrofis. Ser. Conf., 20, 249
Harrison, T. E., Howell, S. B., Szkody, P., Homeier, D., Johnson, J., & Osborne, H. L. 2004c, ApJ, 614, 947
Harrison, T. E., McNamara, B. J., Szkody, P., & Gilliland, R. L. 2000, AJ, 120, 2649
Harrison, T. E., Osborne, H. L., & Howell, S. B. 2004d, AJ, 127, 3493 (Paper I)
Hauschildt, P. H., Allard, F., & Baron, E. 1999, ApJ, 512, 377
Hinkle, K., Wallace, L., & Livingston, W. 1995, PASP, 107, 1042
Hjellming, M. S., & Taam, R. E. 1991, ApJ, 370, 709
Howell, S. B. 2001, PASJ, 53, 675
Howell, S. B., Nelson, L. A., & Rappaport, S. 2001, ApJ, 550, 897
Howell, S. B., Harrison, T. E., & Szkody, P. 2004, ApJ, 602, L49
Jameson, R. F., King, A. R., & Sherrington, M. R. 1980, MNRAS, 191, 559
Kraft, R. P., Sneden, C., Smith, G. H., Shetrone, M. D., & Fulbright, J. 1998, AJ, 115, 1500
Long, K., & Gilliland, R. L. 1999, ApJ, 511, 916
Marks, P. B., & Sarna, M. J. 1998, MNRAS, 301, 699
Mateo, M., Bolte, M., & Szkody, P. 1985, PASP, 97, 45
Mauche, C. W., Lee, Y. P., & Kallman, T. R. 1997, ApJ, 477, 832
Mukai, K., & Charles, P. A. 1987, MNRAS, 226, 209
Osborne, H. L., Harrison, T. E., Howell, S. B., Johnson, J. J., & Gelino, D. M. 2002, AAS Meeting 200, 75.10
Pilachowski, C. A., Sneden, C., Kraft, R. P., & Langer, G. E. 1996, AJ, 112, 545
Ritter, H., & Kolb, U. 2003, A&A, 404, 301
Schenker, K., King, A. R., Kolb, U., Wynn, G. A., & Zhang, Z. 2002, MNRAS, 337, 1105
Schwope, A. D., Beuermann, K., Jordan, S., & Thomas, H.-C. 1993, A&A, 278, 487
Schwope, A. D., Beuermann, K., & Thomas, H.-C. 1990, A&A, 230, 120
Shafter, A. W. 1983, Ph.D. thesis, Univ. California, Los Angeles
Shafter, A. W., & Harkness, R. P. 1986, AJ, 92, 658
Silber, A. D., Raymond, J. C., Mason, P. A., Andronov, I. L., Borisov, N. V., & Shakhovskoy, N. M. 1996, ApJ, 460, 939
Smak, J. I. 2001, Acta Astron., 51, 279
Southwell, K. A., Still, M. D., Connon Smith, R., & Martin, J. S. 1995, A&A, 302, 90
Szkody, P., Raymond, J. C., & Capps, R. W. 1982, ApJ, 257, 686
Wallace, L., Hinkle, K., & Bernath, P. 1996, ApJS, 106, 165
Watson, C. A., Dhillon, V. S., Rutten, R. G. M., & Schwope, A. D. 2003, MNRAS, 341, 129